

## COMPUTER SIMULATION AND TEST BED PERFORMANCE OF A VARIABLE FILL HYDRAULIC DYNAMOMETER

J.K. RAINE and P.G. HODGSON

Department of Mechanical Engineering, University of Canterbury  
 Private Bag, Christchurch, NEW ZEALAND

### ABSTRACT

An analytical model of the steady state and dynamic torque absorption processes in variable fill hydraulic dynamometers is outlined. The model has been developed to simulate the dynamic behaviour of Froude-type dynamometers under open-loop control and of an engine/dynamometer system under various closed-loop control modes. Model predictions for characteristic running full torque absorption performance are compared with test bed results. The influence of vane angle and working fluid properties is described. Numerical solution of the system equations is used in the time-dependent engine/dynamometer dynamic simulation, which reproduces both the negative torque-speed characteristic and other transient phenomena which occur under real open-loop partial fill conditions. Aspects of system closed-loop control are introduced.

### NOTATION

D	outside diameter of rotor cups ( $= 2R_o$ ), m
i	inlet
$J_e$	polar moment of inertia of engine rotating parts, $\text{kgm}^2$
$J_p$	polar moment of inertia of dynamometer rotor, $\text{kgm}^2$
k	shaft torsional stiffness, $\text{Nm/rad}$
$k_t$	torque coefficient, $\text{Nm}/(\text{rev}^2\text{m}^5/\text{min}^2)$
$K_j$	geometrical coefficients, $K_1, K_2, K_3, K_4, K_5, K_6$
$K_c$	proportional gain
N	rotational speed, $\text{rev/min}$
$N_o$	cup emptying speed, $\text{rev/min}$
o	outlet
Perf	volume percentage fill
$Q_i$	inflow rate of water to working compartment, $\text{m}^3/\text{s}$
$Q_o$	outflow rate of water from working compartment, $\text{m}^3/\text{s}$
$R_{ci}$	inner radius of air-water interface, m
$R_{co}$	outer radius of air-water interface, m
$R_i$	working compartment cup inner radius, m
$R_m$	radius of vortex centre from axis of rotor rotation, m
$R_o$	working compartment cup outer radius, m
T	Dynamometer torque, Nm
$T_e$	Engine driving torque, Nm
us	unsteady or time dependent
t	vane thickness, m
$V_f$	volume of working compartment, $\text{m}^3$
VP	water outlet valve position
z	number of vanes
$\alpha$	vane angle relative to plane of rotation of rotor
$\delta$	angular twist of shaft between engine and dynr.
$\rho$	fluid density, $\text{kg/m}^3$
$\omega$	vortex angular velocity, $\text{rad/s}$
$\omega_e$	engine angular velocity, $\text{rad/s}$
$\omega_p$	rotor angular velocity, $\text{rad/s}$
$\dot{\omega}_p$	rotor angular acceleration, $\text{rad/s}^2$

### 1. INTRODUCTION

Hydraulic dynamometers have for a long time been the preferred device for testing of engines under rapid speed and torque transients, particularly in the area of high power internal combustion engine testing, owing to their high torque absorption capacity per

unit rotational inertia. Direct digital control systems are now available for hydraulic dynamometers and this will help the development of self-tuning control algorithms to handle the non-linear characteristics of engine-dynamometer systems.

Studies of fluid coupling performance are well represented in the literature, as reviewed by Hodgson (1991), but there is little reported research into variable fill dynamometers. Work such as that of Narayan Rao (1968) has focused on running full performance without consideration of transient behaviour, or the control system employed. The model of a Froude dynamometer outlined here is described in more detail elsewhere by the Raine & Hodgson (1991, 1992a). The model briefly described here accurately simulates both running full and partial fill behaviour, both for steady state and dynamic operating conditions. The model has also been extended to include both hydromechanical back pressure valve and electrohydraulic servo closed-loop control systems (Hodgson & Raine, 1992b).

### 2. THE TORQUE ABSORPTION PROCESS AND STABILITY

Figure 1 shows a schematic section through a Froude-type variable fill dynamometer. The  $45^\circ$  vaned rotor pumps water from its periphery to the stator cups, which return the flow to the inner diameter of the rotor. The consequent toroidal vortex action gives very effective angular momentum transfer between rotor and stator, and therefore a torque reaction (normally measured by load cell) between the trunnion bearing-mounted machine casing and ground. Passages in the stator vanes feed inlet water to the centre of the toroidal vortex, or vent the centre of the vortex to atmosphere. Pressure generated by the vortex action discharges water at the rotor outside diameter, or through holes at the back of the rotor or stator cups (see Figure 1). The location of the water outlet holes affects the torque absorption characteristics under partial fill.

At steady state, water inflow ( $Q_i$ ) and outflow ( $Q_o$ ) rate are equal and the cup fill is constant. Accelerated from rest, the dynamometer running full absorbs torque along its maximum hydraulic capacity torque-speed curve. Without feedback control continually adjusting the water outlet valve position, a cup emptying speed,  $N_o$ , is reached where the machine pumps water out faster than the rate of inflow. Above speed  $N_o$ , fill decreases with increasing speed. The gradient of this section of the open-loop torque-speed curve depends on the working compartment geometry, but may be strongly negative.

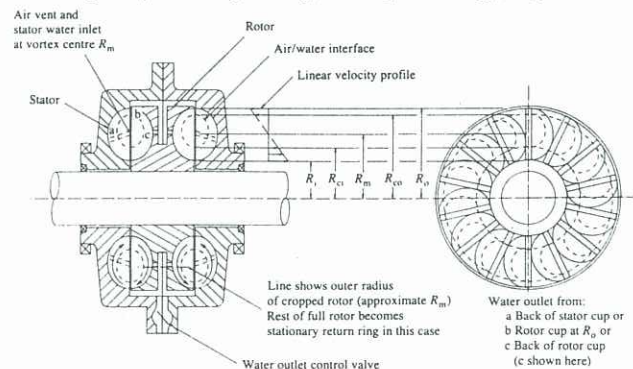


Fig. 1: Schematic section of dynamometer with end view of rotor



The shape of the dynamometer torque-speed curve affects the stability of operation of the engine-dynamometer system. A series of rising dynamometer torque curves (see Fig. 2) will generally intersect I.C. engine torque curves such that  $dT/dN$  is greater for the dynamometer than for the engine, giving stable set point holding. Figure 3 shows that a falling open-loop torque curve on the dynamometer can intersect a typical engine torque curve such that  $dT/dN$  is less for the dynamometer than for the engine. With no mechanism (such as an engine speed governor) to hold the system at its set point, an upwards perturbation in speed results in engine torque exceeding dynamometer torque with consequent uncontrolled acceleration and loss of dynamometer fill. A downwards perturbation in speed causes dynamometer torque to exceed engine torque with consequent deceleration and possible stalling of the engine. For the system model to behave consistently with test bed performance data, the dynamics of the engine must be included as part of the overall system. The model described here includes an engine as an idealised power source with inertia, and capable of uniform, stepped, ramped, sinusoidal and other specified torque and speed characteristics.

### 3. THEORETICAL MODEL

#### 3.1 Basic Equations for Torque and Energy Dissipation

The very extensive mathematical treatment required in the development of the model is described fully by Hodgson (1991). Advances on previous analyses (all steady state except Tan (1980)) include the determination of the of the water outflow rate, the air-water interface radii,  $R_{co}$  and  $R_{ci}$ , under variable fill conditions, conditions for equilibrium between water inflow and outflow, and an accurate expression for working compartment pressure. The steady state and dynamic models utilise an integrated one-dimensional analysis in which general non-steady state equations are developed for the conservation of mass, torque, energy dissipation and cup vortex pressure, percentage fill and cooling water mass outflow rate. Space allows only a few key equations to be summarised below in abbreviated form. General non-steady state torque is given by

$$T_{us} = K_1 \omega \omega_p + K_2 \omega^2 + K_3 \omega_p + K_4 \omega + K_5 \dot{\omega}_p + K_6 \dot{\omega} \quad (1)$$

The first two terms of Equation 1 are the steady state torque while the last four terms handle the additional torque components due to unsteady speed and fill. The constants  $K_i$  are functions of working fluid density and the working compartment geometry, of the form

$$K_j = f(\rho, R_o, R_{co}, R_m, R_{ci}, R_i, \alpha, z, t) \quad (2)$$

The dimensions of the  $K_i$  equations are such that Equation 1 satisfies hydrodynamic machine similarity laws. To determine dynamometer torque from Equation 1, the vortex angular velocity,  $\omega$ , must be determined. This is done by equating the rotational power input to the rate of conversion from kinetic energy to fluid internal energy in the toroidal vortex. Three energy dissipation mechanisms are included: incidence or shock loss as the water passes from one component to another, friction loss along vane and wall surfaces and secondary circulation losses. The final energy dissipation equation is

$$T_{us} \omega_p = K_{11} \omega \omega_p^2 + K_{12} \omega^2 \omega_p + (K_{13} + K_f + K_{sc}) \omega^3 \quad (3)$$

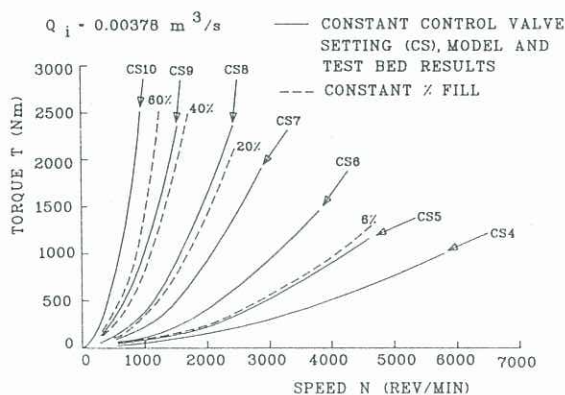


Fig. 2: Torque-speed characteristics at constant control valve settings for F24 dynamometer with back pressure valve control

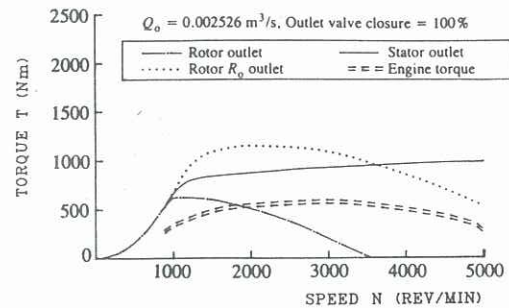


Fig. 3: Simulated steady state torque-speed curves for F0201 variable fill dynamometer

This gives a quadratic equation which can easily be solved for  $\omega$ , the vortex circulation angular velocity. In general, the lower the values for the  $K_i$ ,  $K_f$ , and  $K_{sc}$  coefficients for incidence, friction and secondary circulation respectively, the higher will be the vortex angular velocity for a given rotor speed and the higher the torque absorption per unit rotor diameter. The expression for vortex pressure is a function of working compartment geometry, the rotor angular velocity,  $\omega_p$ , the vortex angular velocity,  $\omega$ , the percentage fill, and the position on the working compartment wall. The computer model can be run with a constant percentage fill, i.e.  $R_{co}$  and  $R_{ci}$  fixed, to generate torque speed curves as illustrated in Figure 2. This requires the water outlet valve position to vary with machine speed to maintain  $Q_o = Q_i$ . Under dynamic conditions, e.g. speed and/or torque transients,  $Q_o$  does not in general equal  $Q_i$ .

#### 3.2 Dynamic Open-Loop Simulation

The engine/dynamometer system is modelled as a two rotor system connected by a drive shaft of torsional stiffness,  $k$ . Engine torque is the forcing function, although engine speed can also be manipulated to represent engine speed control. The dynamometer is represented as a rotary power dissipator (damper) with a non-linear reaction torque characteristic and variable fluid fill. By reducing the two second order governing equations to four first order equations and considering the relative angular displacement,  $\delta$ , between the rotors, the system is represented by four differential equations:

$$\dot{\delta} = \omega_b - \omega_p \quad (4)$$

$$J_e \dot{\omega}_b = T_e - k \delta \quad (5)$$

$$J_p \dot{\omega}_p = k \delta - T \quad (6)$$

$$\frac{d}{dt} (\text{Perf}) = \frac{1}{V_i} (Q_i - Q_o) \quad (7)$$

Equation 7 assumes constant density for the working fluid. As the equations for torque, air-water interface radii, vortex pressure and water outflow are very non-linear, the system equations are solved numerically in terms of the variables  $\delta$ ,  $\omega_b$ ,  $\omega_p$ , and Perf. To control dynamometer torque or speed, the only directly controllable inputs are outlet valve position VP (therefore  $Q_o$ ), and water inflow rate,  $Q_i$ .

For the dynamic computer simulation, the system equations for torque, energy dissipation and pressure are used to evaluate dynamometer parameters in Equations 4 to 7 at each time point, as time steps forward, and thus the values of the differential equations. These numerical values are used to solve the system of equations forward in time. This is a typical initial value problem, solved using the Adams Predictor Corrector Method as presented by Shampine and Gordon (1975) and described in detail by Hodgson (1991).

#### 3.3 Dynamic Closed Loop Simulation

While there are several ways of achieving stable closed-loop control, two methods used on Froude dynamometers were modelled by the authors (1992b) and results compared with test bed performance: (i) a hydromechanical back pressure valve at the water outlet which closes with increasing speed to achieve approximately constant fill for any one control setting, thus continuously rising torque speed curves, and (ii) an electrohydraulically actuated PID servo-controlled water outlet butterfly valve, using speed or torque feedback, or both, to provide constant-speed, constant-torque, or a propeller law torque-speed characteristic respectively. Control equations for these two systems are described by Hodgson (1991). The control equations are combined with the dynamic open-loop model to give appropriate complete closed-loop computer models.



## 4. MODEL AND EXPERIMENTAL RESULTS

### 4.1 Running Full Performance

The dynamometer model equations were utilised in a FORTRAN 77 computer program which simulates the engine-dynamometer system. Initially the program was used to predict running full performance and effects of changes to working compartment geometry. Figure 4 shows a dimensionless plot of maximum hydraulic capacity torque curves for a family of geometrically similar dynamometers. Results are non-dimensionalised using the relationship  $T_{max} = k_1 N_o^2 D^5$ . The model prediction is shown for comparison. Once scaled to a reference real machine by setting the secondary circulation loss coefficient,  $K_{sc}$ , the model may be used to predict the maximum torque for variations of the basic machine geometry such as working compartment diameter, vane angle and thickness, or surface roughness. Plots similar to Figure 4, with excellent agreement between model and test bed results, may be produced for other machines such as cropped rotor high speed dynamometers (Raine & Hodgson, 1991).

A study of the variation in running full maximum torque with vane angle (Raine & Hodgson, 1991) predicts an optimum vane angle of  $39^\circ$  to the rotor plane, and an optimum inlet angle of  $35^\circ$  for helical twisted vanes with the outlet angle held at  $39^\circ$ . Variation in cup surface roughness height from 0.127 mm (as-cast) to 0.0127 mm (polished) results in a useful predicted 19% increase in maximum torque  $T_{max}$  on a dynamometer with 200 mm diameter rotor. Table 1 shows the effect of working fluid properties predicted by the model.

Table 1: Influence of fluid density and viscosity on  $T_{max}$  at 1500 rev/min for a dynamometer with 200 mm diameter rotor

Fluid	Density $kg/m^3$	Viscosity $m^2/s$	Friction factor $f$	Torque Nm
Water	998.20	1.14E-6	0.02013	1425.00
Auto Trans Oil	863.4	3.52E-5	0.02014	1233.00
SAE 20W/50	891.4	1.58E-4	0.02016	1272.00

### 4.2 Steady State Variable Fill Performance

Sample results of steady state variable fill performance are shown in Figures 2 and 3. The dotted torque-speed curves in Figure 2 are for constant percentage partial fill. Figure 3 shows simulated steady state torque speed curves for an F0201 dynamometer with 200 mm dia. rotor and different working compartment water outlet positions.

In the partial fill zone, off the maximum torque-speed curve, the dynamometer tries to self-empty in regions where  $dT/dN$  is less for the dynamometer than for the engine, and a simulated quasi steady-state is imposed by holding the dynamometer at each speed and letting the fill adjust to achieve a vortex pressure which makes  $Q_i = Q_o$ , and a value of  $\omega$  which sets energy dissipation at a rate equal to

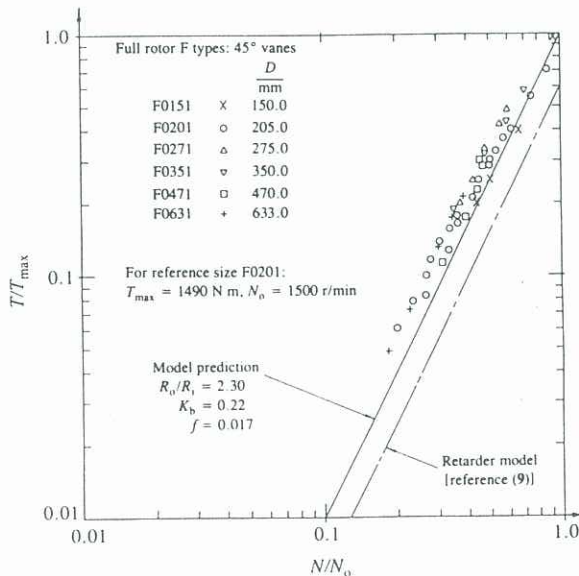


Fig. 4: F-type dynamometer maximum hydraulic capacity torque

the input power  $T\omega_p$ . Figure 3 shows that when the water outlet is from the back of the rotor cups or rotor cup outside diameter, the dynamometer is strongly self-emptying and displays a falling torque curve. This is due to recovery of absolute velocity head from the working compartment vortex increasing discharge pressure at the outlet valve. Without the effect of the rotor's centrifuging action, the discharge pressure is lower for a stator cup outlet, which gives a more desirable steady state torque curve with no negative gradient.

### 4.3 Dynamic Open Loop Performance

Results in this and subsequent sections refer to an F24 dynamometer, of 240 mm nominal rotor diameter and  $0.20 kgm^2$  rotor inertia. Figure 5 shows the effect of acceleration on the simulated torque-speed curve of the dynamometer. A series of simulated accelerations is compared with test bed data at various water outlet valve openings. The effect of acceleration is to carry the torque further up its maximum hydraulic capacity curve before cup emptying occurs, with a subsequent fall in torque as fill decreases. This effect results from a finite time being needed for working fluid to accelerate and produce a higher vortex pressure then an adjustment in fill. The model was run at a constant acceleration rate of 500 rev/min/s, whereas the test bed data were obtained using a variable speed drive whose rate of acceleration was not constant. Nonetheless, the model results show very good agreement at moderate outlet valve closures.

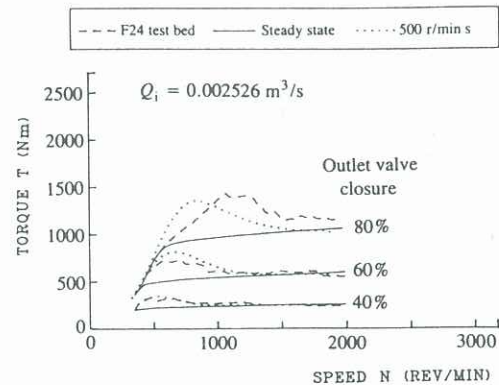


Fig. 5: Comparison of steady state and dynamic model torque-speed curves with test bed accelerations at various outlet valve percent closures

Hodgson & Raine (1992a) present other torque-speed curves demonstrating fluid dynamical inertia effects simulated by the model during acceleration and deceleration of the dynamometer. Good agreement is achieved between model and test bed results in regard to (i) the false maximum torque curve that can occur at 100% outlet valve closure on acceleration from an initial fill less than 100%, (ii) the real hysteresis that occurs between acceleration and deceleration torque curves at a fixed outlet valve setting. The model also demonstrates the rise in torque that occurs in practice at high speed following a falling torque region under open-loop control.

A final result from the open-loop modelling is shown in Figure 6, which shows transients for 10% and full outlet valve closure (100% valve closure takes 200 ms) from the initial point 339 Nm and 1200 rev/min. It is seen that while the 10% closure moves to a new steady state within about 0.5 second, closing the valve fully rapidly forces the dynamometer towards 100% fill and a torque in excess of the rated torque of the machine. In general the dynamometer will reach rated torque more rapidly the higher the initial torque and the higher the speed at which the transient occurs. Data for an open-loop torque transient on an F24 provided by Dukes (1991) show an average rate of torque application on an F24 dynamometer of 3750 Nm/s for a 100% outlet valve closure from no load at 1950 rev/min, and a peak rate of torque increase of 6500 Nm/s (see Figure 6).

### 4.4 Dynamic Closed Loop Performance

All model and test bed results assume an engine rotating inertia of  $0.2 kgm^2$ . In Figure 2 it is seen that the back pressure valve closed-loop control imposes a set of square law torque-speed curves at any control setting, approximating lines of constant fill. This form of control can offer a reasonably fast response to a given engine torque transient along a constant control valve setting characteristic, but will generally be slower to reach a new set point than electrohydraulic servo-control. It offers a low cost means of



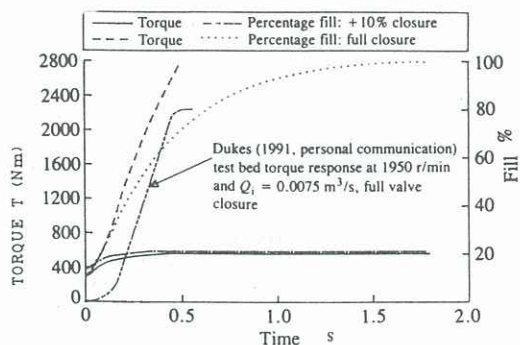


Fig. 6: Dynamometer response to +10% and full valve closure at 1200 r/min constant speed

stable steady state testing of ungoverned engines where fast transient response is not required. The model accurately simulates test bed behaviour. Hodgson & Raine (1992b) give results for transients where both engine torque output and dynamometer control setting are changed simultaneously.

The electrohydraulic servo-control uses a digital velocity form of the PID equation. As the system model is very non-linear, an empirical technique (Stephanopoulos, 1984) is used to tune the control parameters while preserving the non-linear behaviour of the dynamometer as the set point moves across the dynamometer operating envelope. Figure 7 shows the system response to a 25% increase in engine input torque with the dynamometer in constant speed control mode. The system behaviour is quite different from open-loop control which results in working compartment self-emptying and uncontrolled acceleration. Figure 7 also shows that to obtain acceptable transient response, the proportional gain,  $K_c$ , needs to be increased substantially above its base value. In the form of the digital PID equation used, modification to  $K_c$  also modifies the integral (I) and rate (D) terms (Hodgson & Raine, 1992b).

A final result is shown in Figure 8. Here a 2 litre Ford Cosworth engine is accelerated from idle, about 800 rev/min, to a demand speed of 6,000 rev/min at 4,000 rev/(min.s) (dynamometer in constant-speed control mode) with an engine torque transient of 210 Nm. After tuning of the PID control parameters agreement between model and test bed results is acceptable, given the simulation of the non-linear engine torque transient as a linear change at 300 Nm/s.

## 5. CONCLUSION

This paper has given an overview of the ability of a dynamic engine/hydraulic system model to simulate real performance. Other uses include modelling the performance of the variable fill dynamometer as a torsional vibration damper. The non-linear system behaviour and consequent need for variable PID servo-control parameters indicate that for optimal control, development of an adaptive self-tuning control algorithm would offer convenience and an improvement in system transient performance and easier adaptation to different engine torque-speed characteristics.

## 6. ACKNOWLEDGEMENT

Figures and extracts from Raine and Hodgson (1991), and Hodgson and Raine (1992a and 1992b) are reproduced by permission of the Council of the Institution of Mechanical Engineers, London, England.

## 7. REFERENCES

- DUKES, B.J. (1991) Personal communication with the authors. Froude Consine Limited, Worcester England.
- HODGSON, P.G. (1991) Theoretical model and dynamic simulation of a hydraulic dynamometer. Ph.D. Thesis, University of Canterbury, Christchurch, N.Z.
- HODGSON, P.G. AND RAINE, J.K. (1992a) Computer simulation of a variable fill hydraulic dynamometer. Part 2: steady state and dynamic open loop performance. *Journal of Mech. Eng. Science*, IMechE, Vol.206, pp49-56.
- HODGSON, P.G. AND RAINE, J.K. (1992b) Computer simulation of a variable fill hydraulic dynamometer. Part 3: closed-loop performance. Accepted for publication in *Journal of Mech. Eng. Science*, IMechE, Vol. 206.

NARAYAN RAO N.N. (1968) The basic theory of hydraulic dynamometers and retarders. *Trans. SAE*, v77, No.680178.

RAINE, J.K. AND HODGSON, P.G. (1991) Computer simulation of a variable fill hydraulic dynamometer. Part 1: torque absorption theory and the influence of working compartment geometry on performance. *Jnl of Mech. Eng. Science*, IMechE, Vol.205, pp155-163.

SHAMPINE, L.F. AND GORDON, M.K. (1975) *Computer solution of ordinary differential equations - the initial value problem*. Freeman & Co., San Francisco.

STEPHANOPOULOS, G. (1984) *Chemical Process Control*. Prentice Hall, Englewood Cliffs, New Jersey.

TAN, K.C. (1980) Identification of an hydraulic dynamometer. M.Sc. thesis, UMIST, England.

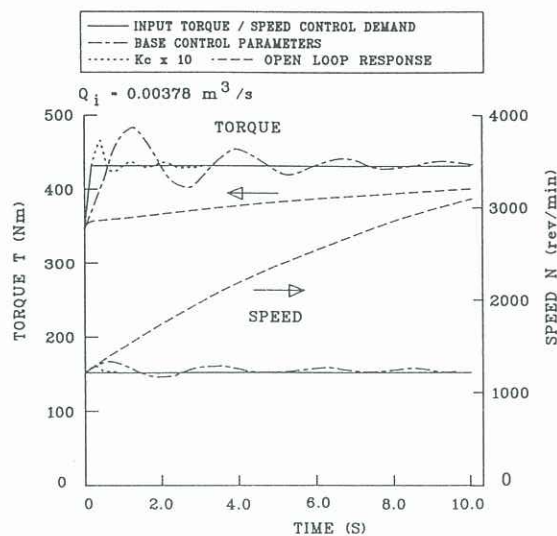


Fig. 7: Transient response to +25% input torque change in dynamometer constant speed mode

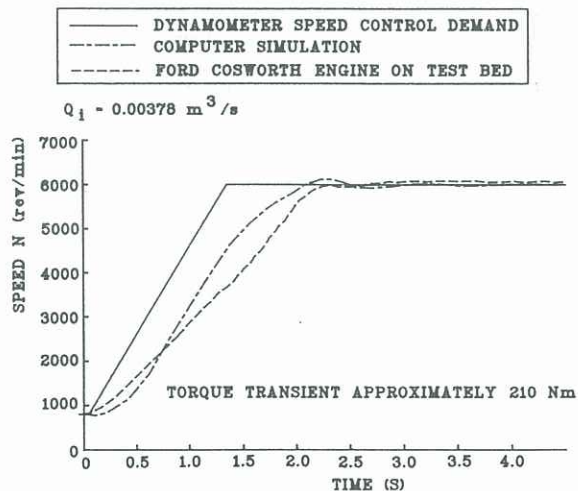


Fig. 8: Comparison of simulated and real transient response to changes in both input torque and dynamometer speed control demand